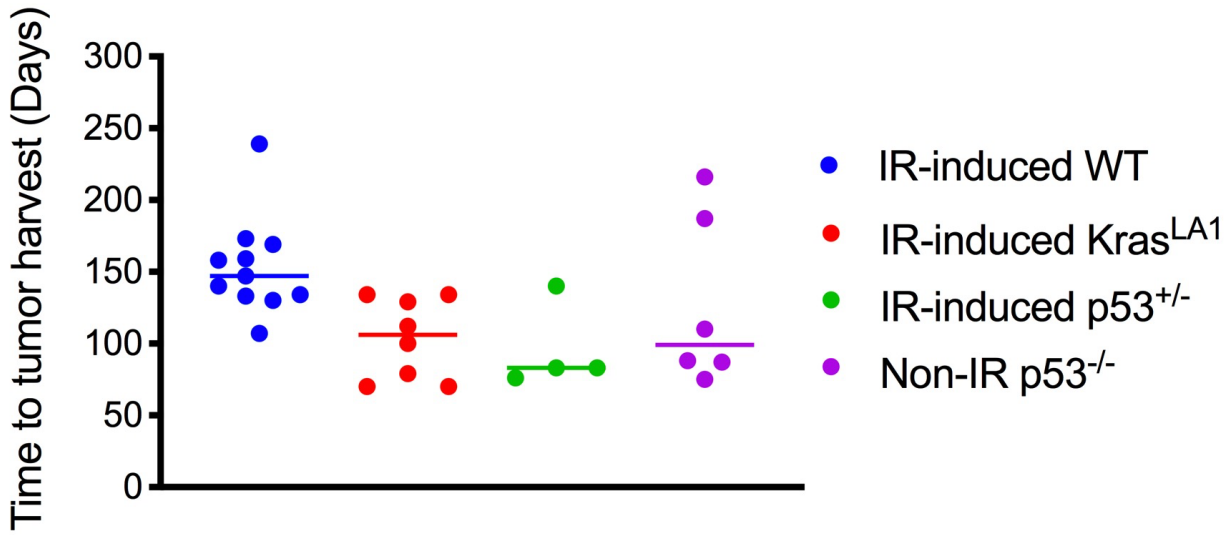

Figure S1. The latency period of thymic lymphomas from irradiated and unirradiated mice. Radiation-induced thymic lymphomas were generated in wild-type (WT) (C57BL/6J) mice, Kras^{LA1} mice or p53$^{+/-}$ mice that were exposed to 1.8 Gy total-body irradiation (TBI) per week for 4 consecutive weeks. Unirradiated Tie2Cre; p53$^{FL/-}$ mice (Non-IR p53$^{-/-}$) in which both alleles of the p53 gene are deleted in endothelial cells and hematopoietic cells were used to generate thymic lymphomas in the absence of irradiation. For IR-induced WT, IR-induced Kras^{LA1} and IR-induced p53$^{+/-}$ mice, data represent the number of days after exposure to 1.8 Gy x 4 TBI. For Non-IR p53$^{-/-}$ mice, data represent the number of days after the mice reached 7 weeks old. Data are presented as dot plots with median. Each dot represents one tumor.

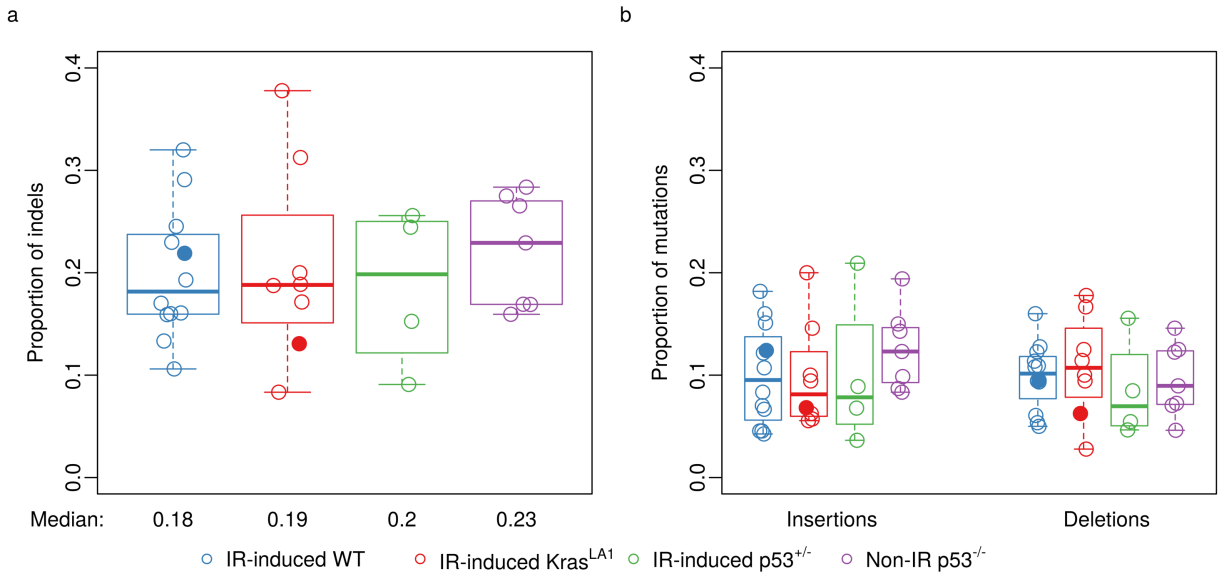

Figure S2. The distribution of sequence variants within total (synonymous and nonsynonymous) somatic mutations. **a,** The proportion of insertion-deletions (indels) within total mutations. **b,** The proportions of insertions and deletions within total mutations. Data from lymphomas that had a substantially higher number of somatic mutations (5015 and 5020) were denoted by closed circles.

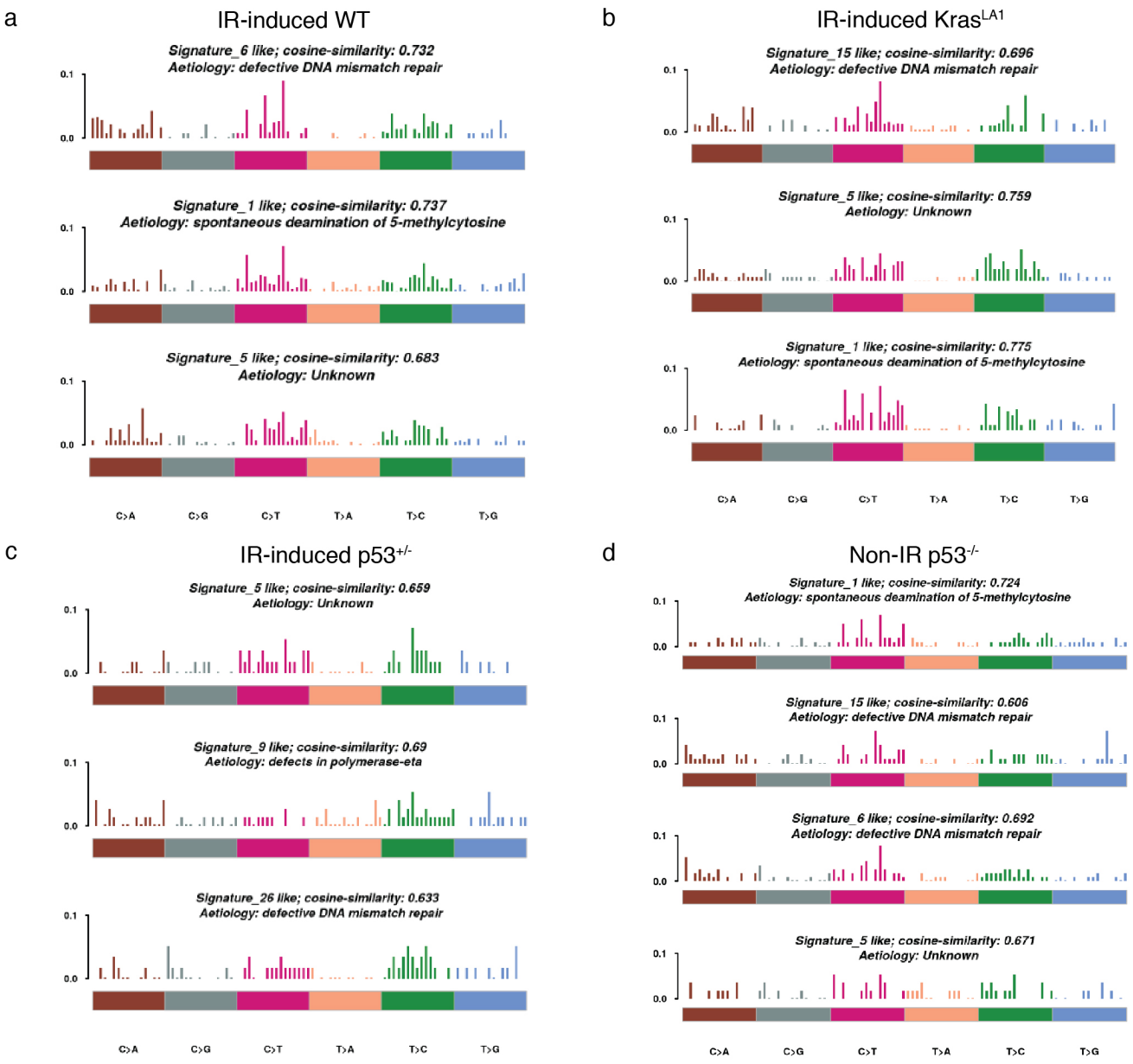

Figure S3. Mutational signature analysis of thymic lymphomas. Mutational signatures of each lymphoma genotype were generated using nonnegative matrix factorization (NMF) trinucleotide-based analysis. From each lymphoma genotype, either 3 or 4 individual signatures were generated. Each murine lymphoma signature was compared to COSMIC mutational signatures of human cancers to identify the COSMIC signature with the highest cosine-similarity score.

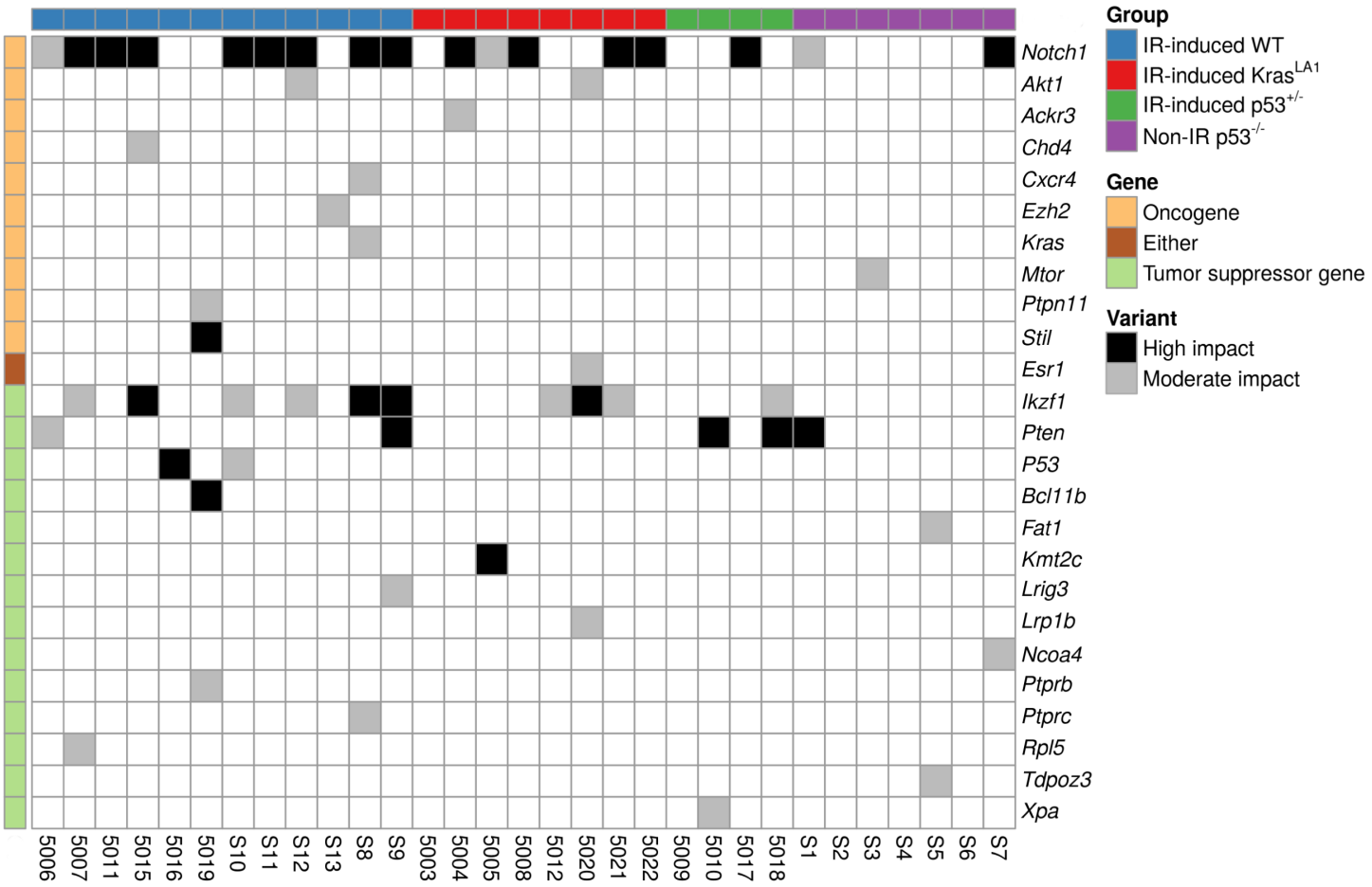

Figure S4. All nonsynonymous mutations in COSMIC genes across thymic lymphomas. Of note, 90% (18/20) of IR-induced WT and IR-induced Kras^{LA1} lymphomas did not harbor mutations in p53. Among lymphomas that retained functional p53, approximately 83% (15/18) of these tumors harbored mutations *Notch1* and/or *Ikzf1*. Three p53 WT lymphomas that did not harbor mutations in either *Notch1* or *Ikzf1* are 5019 (mutations in *Ptpn11*, *Stil*, *Bcl11b* and *Ptprb*), S13 (mutation in *Ezh2*) and 5003 (mutation in *Kras*).

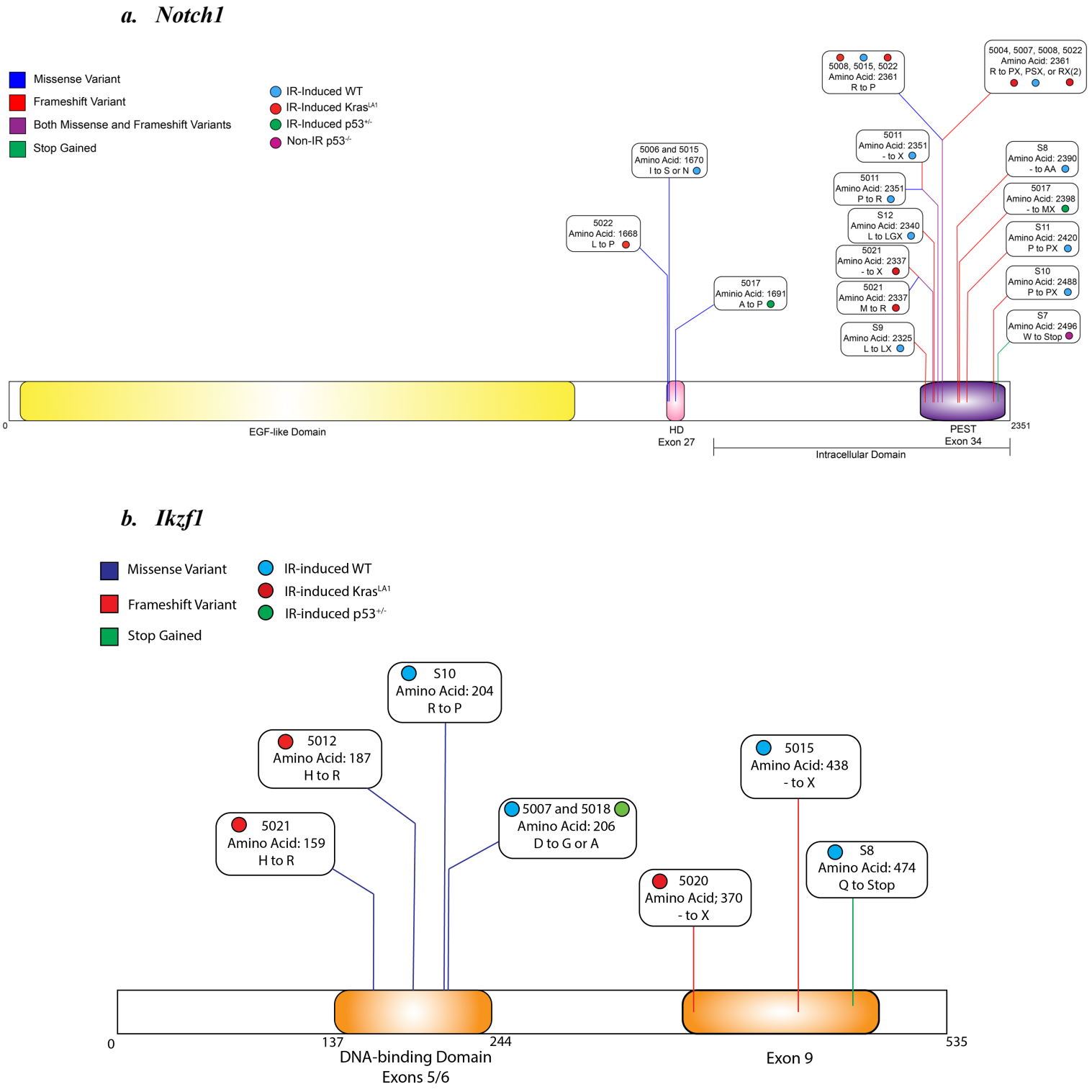

Figure S5. Schematic of nonsynonymous mutations in *Notch1* and *Ikzf*. All mutations listed in the plots were validated by Sanger sequencing. Colors of each dot represent lymphomas from mice with different genotypes. Colors of each line represent different types of somatic mutations. HD: heterodimerization domain; PEST: proline, glutamic acid, serine, threonine-rich domain

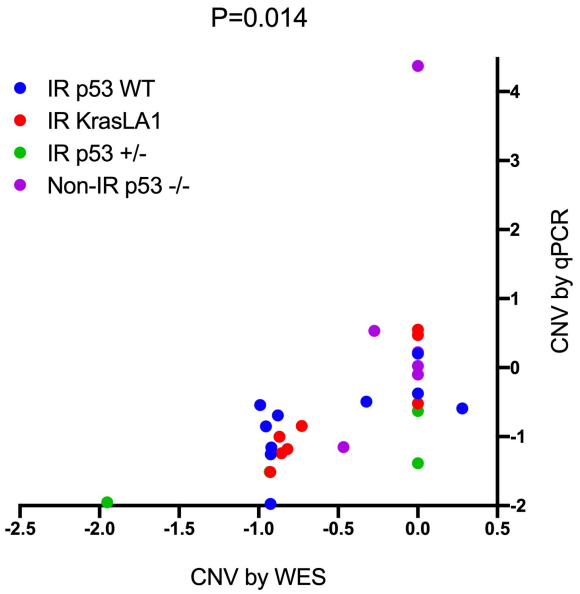

Figure S6. Validation of copy number variations (CNV) of *Ikzf1* determined by whole exome sequencing (WES) using qPCR. qPCR was performed using the same genomic DNA used for WES. *P* value was calculated by Kendall's W test for concordance, corrected for ties.

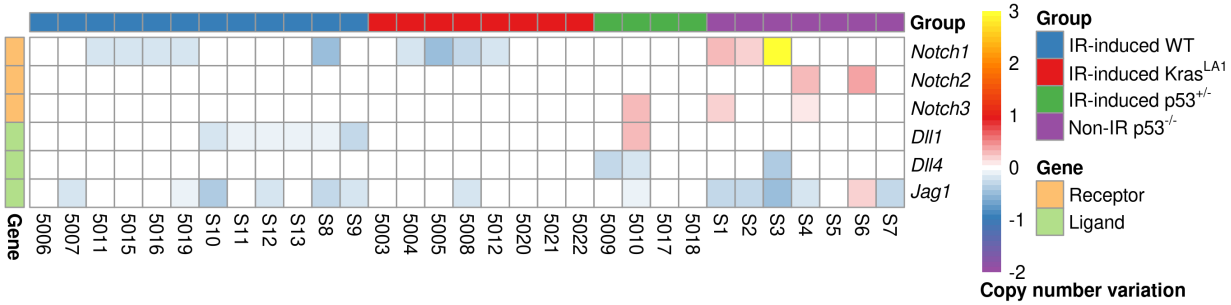

Figure S7. Copy number variations in Notch receptors (*Notch1*, *Notch2* and *Notch3*) and Notch ligands (*Dll1, Dll4* and *Jag1*) across thymic lymphomas.

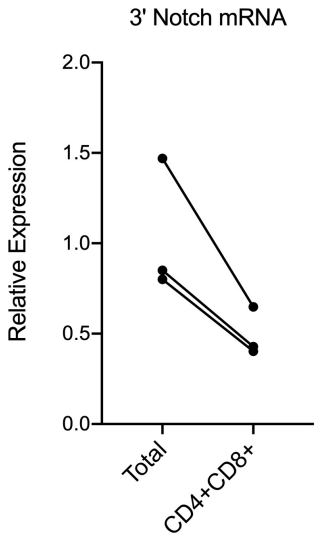

Figure S8. The expression of 3' Notch1 mRNA in $CD4^+CD8^+$ thymocytes compared to total thymocytes. Total thymocytes were harvested from unirradiated C57BL/6J mice (n=3 mice). $CD4^+CD8^+$ thymocytes were isolated from total thymocytes by flow sorting. The expression of 3' Notch1 mRNA was assessed in total thymocytes and $CD4^+CD8^+$ thymocytes from the same mouse (n=3 mice).

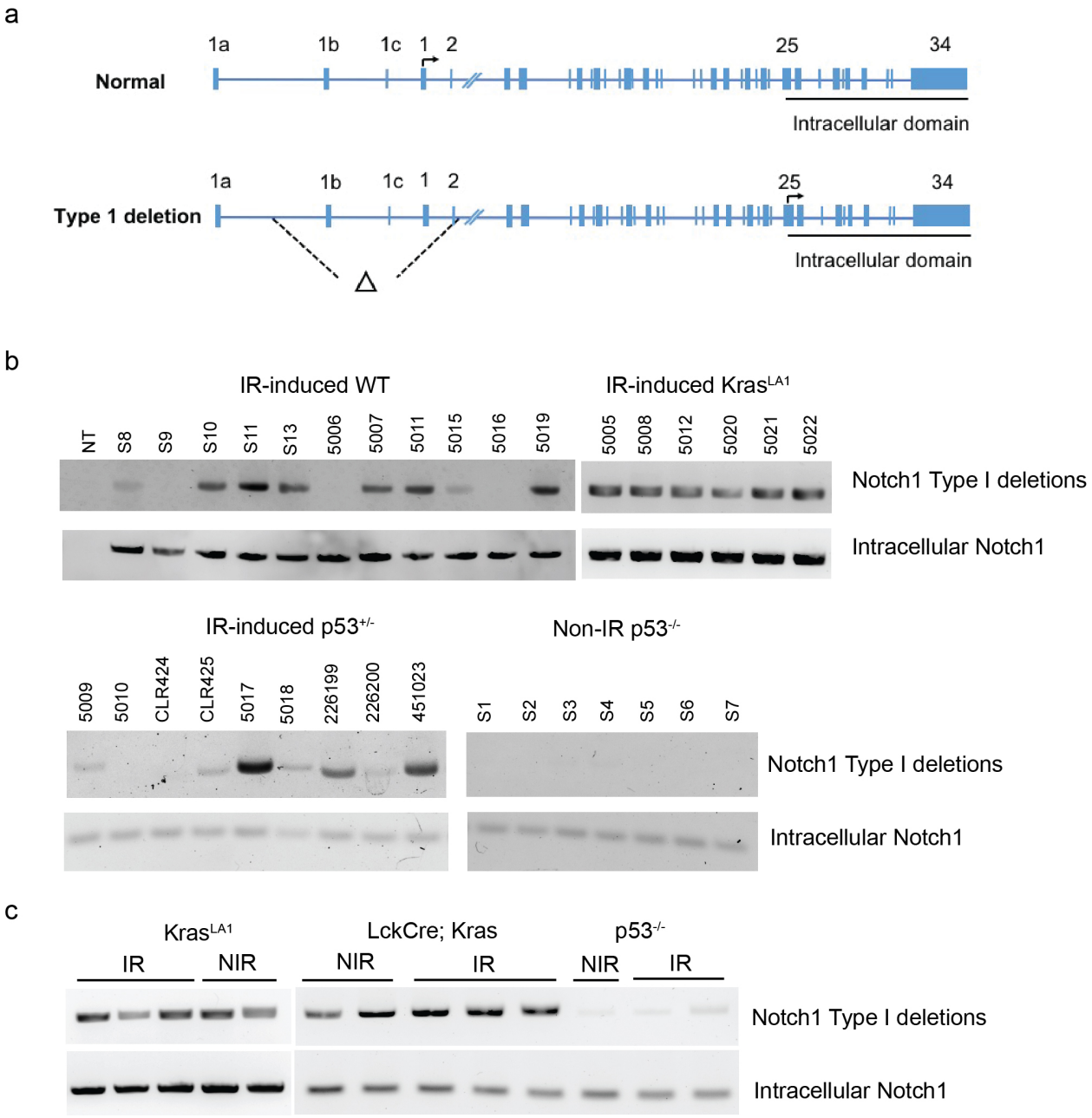

Figure S9. Detection of Type 1 deletions of the *Notch1* gene**. a,** Schematics of Type 1 deletions of *Notch1*. Type 1 deletions remove the 5′ proximal promoter and exon 1 of *Notch1*, which activates transcription from the cryptic promoter in exon 25. **b,** Gel images showing the detection of *Notch1* Type 1 deletion in the genomic DNA by PCR. Amplification of a region inside the intracellular domain was used as a positive control for the presence of genomic DNA. NT, no template. **c,** Detection of Type 1 deletions of the *Notch1* gene in thymic lymphomas from irradiated (IR) and unirradiated mice (NIR) of the same genotype, including $Kras^{LA1}$, LckCre; LSL-$Kras^{G12D}$ and $p53^{-/-}$. Each lane represents one tumor.

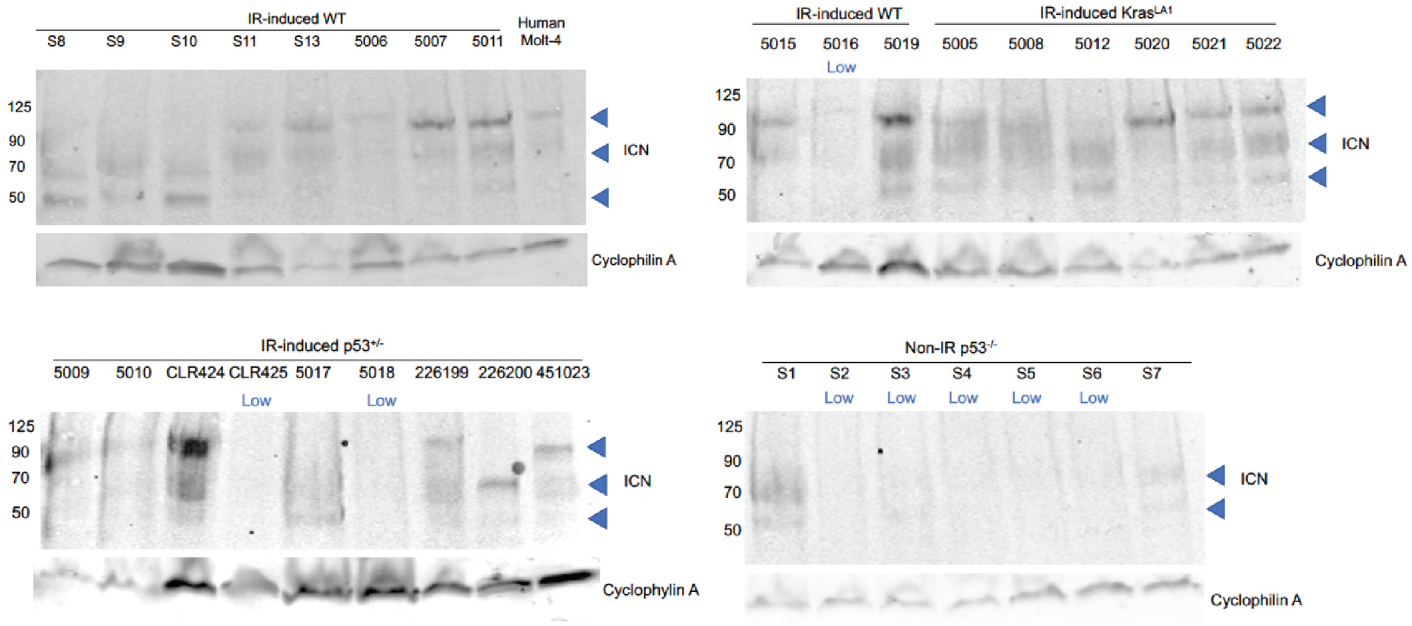

Figure S10. Western blot that detects the expression of intracellular Notch1 (ICN) protein. Of note, we detected ICN proteins with different molecular weights (indicated with blue triangles), which is likely due to different truncation mutations that occurred in the PEST domain of Notch1. Cyclophylin A was used as a control for protein loading. A human T-cell acute lymphoblastic leukemia cell line Molt-4 was used as a control for ICN protein.

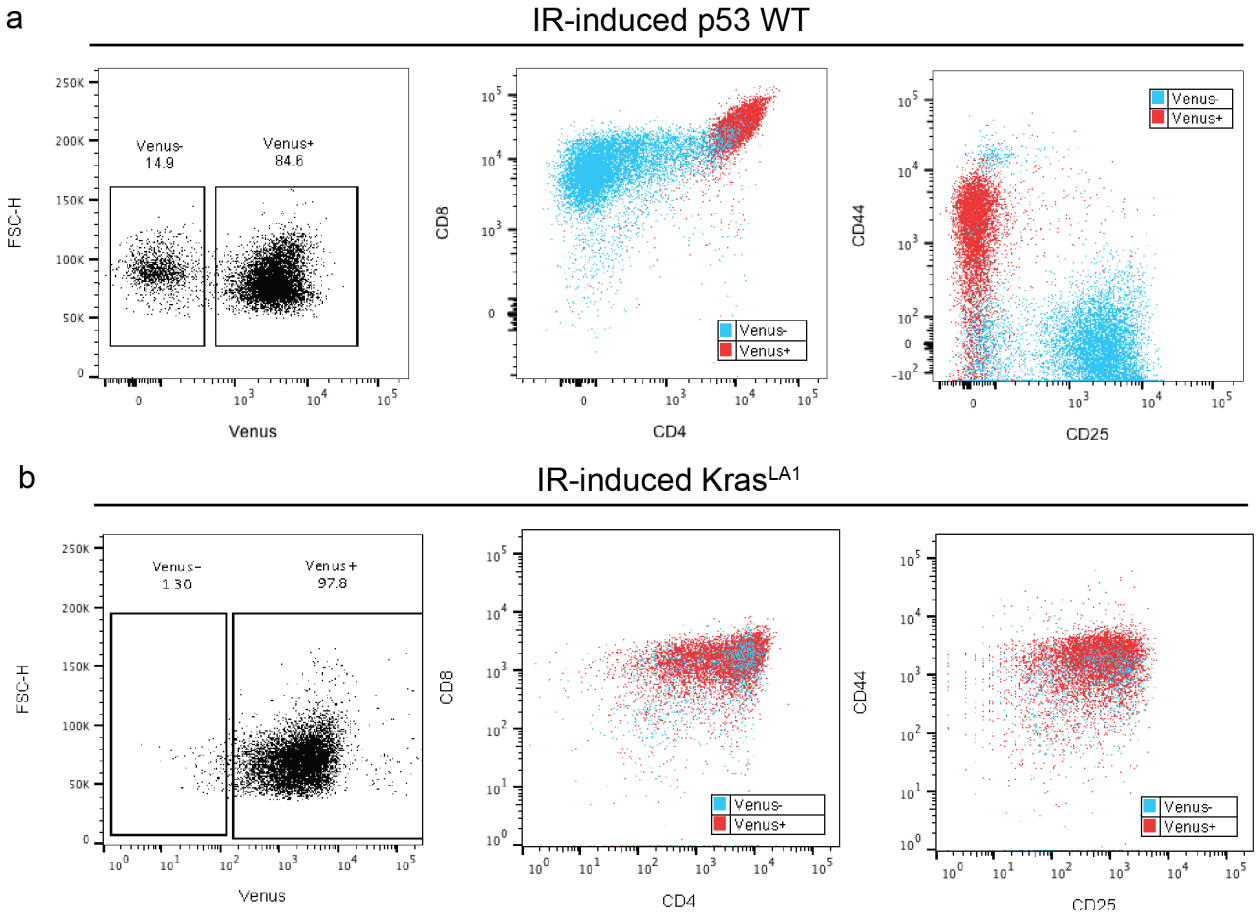

Figure S11. Detection of lymphoma cells exhibiting activated Notch1 signaling using Rbpj-Venus reporter mice. **a-b**, Representative flow cytometry data of radiation-induced thymic lymphoma that developed in Rbpj-Venus reporter mice on a p53 WT or KrasLA1 background. Venus+ cells and Venus- cells are labeled in red and blue, respectively.